The Influence of the Side Chain Length on −OCH3−π Interactions Determining the Crystal Packing of Four Substituted 1,4-Bis(α-styryl)benzenes

ARTICLE *in* CRYSTAL GROWTH & DESIGN · JUNE 2004

Impact Factor: 4.89 · DOI: 10.1021/cg0499764

CRYSTAL GROWTH & DESIGN
2004
VOL. 4, NO. 4
823−830

The Influence of the Side Chain Length on $-OCH_3-\pi$ Interactions Determining the Crystal Packing of Four Substituted 1,4-Bis(α-styryl)benzenes

Christophe M. L. Vande Velde,[†] Li-Juan Chen,[†,‡] Jan K. Baeke,[†] Maarten Moens,[†] Pieter Dieltiens,[†] Herman J. Geise,[†] Matthias Zeller,[§] Allen D. Hunter,[§] and Frank Blockhuys*[,†]

Department of Chemistry, University of Antwerp, Universiteitsplein 1, B-2610 Wilrijk, Belgium, and Structure and Chemical Instrumentation Center, Youngstown State University, One University Plaza, Youngstown, Ohio 44555

Received January 6, 2004; Revised Manuscript Received March 29, 2004

ABSTRACT: The crystal structures of *E*,*E*-1,4-bis[2-(2,4,6-trimethoxyphenyl)ethenyl]-2,5-dimethoxybenzene (**1**), *E*,*E*-1,4-bis[2-(2,4,6-trimethoxyphenyl)ethenyl]-2,5-diisopropoxybenzene (**2**), *E*,*E*-1,4-bis[2-(2,4,6-trimethoxyphenyl)-ethenyl]-2,5-dihexoxybenzene (**3**), and *E*,*E*-1,4-bis[2-(2,4,6-trimethoxyphenyl)ethenyl]-2,5-bis(2-phenylethoxy)benzene (**4**) are reported. A weak intramolecular hydrogen bond between protons on the olefinic link and the *ortho*-methoxy groups on the adjacent benzene rings is commented on. In general, however, the crystal packing for these structures is primarily determined by weak $-OCH_3-\pi$ interactions. Their numbers change with the structure and length of the side chains and with the accommodation of the extended chains in the lattice. A discussion on the effects of these interactions on the possibility of lattice formation explains why these four compounds crystallize and several similar ones with different alkoxy side chains do not.

1. Introduction

This study reports on the crystal structures of a series of substituted 1,4-bis(α-styryl)benzenes. The main focus lies on their crystal packing to identify the structural features that govern their molecular alignment in the solid state. Such information may in the long-term shed light on processes such as molecular aggregation and phase separation, which are important for the efficiency and lifetime of organic light-emitting diodes (OLEDs) based on this type of material, for example.[1−3] Four compounds were selected for an in-depth study, that is, *E*,*E*-1,4-bis[2-(2,4,6-trimethoxyphenyl)ethenyl]-2,5-dimethoxybenzene (**1**), *E*,*E*-1,4-bis[2-(2,4,6-trimethoxyphenyl)ethenyl]-2,5-diisopropoxybenzene (**2**), *E*,*E*-1,4-bis[2-(2,4,6-trimethoxyphenyl)ethenyl]-2,5-dihexoxybenzene (**3**), and *E*,*E*-1,4-bis[2-(2,4,6-trimethoxyphenyl)-ethenyl]-2,5-bis(2-phenylethoxy)benzene (**4**). The main intermolecular interactions determining the crystal packing and causing the molecular alignment of 1,4-bis(α-styryl)benzenes with this particular pattern of methoxy substitution are weak $-OCH_3-\pi$ interactions, as will be expanded on in the rest of the text.

Apart from the relevance of these compounds as optical materials, these lattice-defining $-OCH_3-\pi$ interactions are equally interesting from a fundamentally scientific point of view. The Crystal Structure Database (CSD)[4,5] lists 17 032 structures that contain a methoxy-substituted phenyl ring. Of these, 1114 (6.5%) display a hydrogen atom of a methoxy group lying 2.5−3.0 Å from the face of a phenyl ring at a C−H···Cg angle of 140°−180°, where Cg is the centroid of the phenyl ring. Only 114 compounds contain a 1,3,5-trimethoxyphenyl moiety, but of these, 36 compounds (31.5%) display the same interaction geometry. In most cases, other, stronger interactions determine the packing, but we were able to find at least two examples where $-OCH_3-\pi$ interactions are prominently visible in the structure and also form an intricate network. These are 2,4,6-trimethoxybenzoic acid[6] and 1,3,5-trimethoxy-2-(1-propenyl)benzene.[7] These data suggest that an extended, layered network as we find it in the structures discussed here is a relatively uncommon occurrence.

An interesting publication worth mentioning in the context of the packing of 1,4-bis(α-styryl)benzenes was written by Bartholomew and co-workers recently.[8] The authors present crystal structures of seven distyrylbenzenes substituted with a variety of functional groups. They conclude that the distyrylbenzene moiety is very flexible in its packing behavior and that "it is straightforward to rationalize [the packing] in the light of electrostatic interactions".[8] However, in their series of compounds, known crystal engineering synthons (such as nitro and nitrile groups, perfluoro substitution, and an unsubstituted diphenylethenyl group) are present and substantially facilitate this rationalization process. For the methoxy-substituted distyrylbenzenes presented and reviewed in their article, the lattice-determining interactions are varying CH···O contacts at a distance equal to the sum of the van der Waals radii. Again, a $-OCH_3-\pi$ network is not observed in these structures.

Thus, it is clear that predicting the crystal structure and packing for these and other materials is still not straightforward, but valuable clues can be obtained from the careful study of the packing. In our case the crystal structures are described mainly as a function of the observed $-OCH_3-\pi$ interactions, which are weighted against intramolecular effects obtained from theoretical calculations. On the basis of this description, it can be rationalized that other substituted derivatives with different side chains do not crystallize. Furthermore, the

* Corresponding author. Tel: +32.3.820.23.65. Fax: +32.3.820.23.10. E-mail: Frank.Blockhuys@ua.ac.be.
[†] University of Antwerp.
[‡] On leave from the Chinese Academy of Sciences, 100101 Beijing, China.
[§] Youngstown State University.

10.1021/cg0499764 CCC: $27.50
Published on Web 06/04/2004

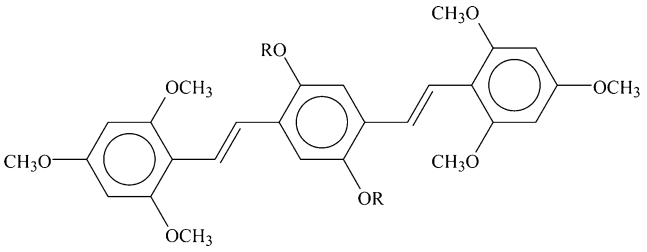

Figure 1. Molecular structures of compounds **1** [R = CH_3], **2** [R = $CH(CH_3)_2$], **3** [R = $(CH_2)_5CH_3$], and **4** [R = CH_2CH_2Ph].

influence of the $-OCH_3-\pi$ interactions on a macroscopic property, that is, the melting point, could also be determined.

2. Experimental Section

The compounds were synthesized according to previously published procedures.[9] X-ray quality crystals of **1** were grown by layering a methylene chloride solution with hexanes. Compound **2** was easily crystallized from hot *p*-xylene in orange needles and compound **3** conveniently crystallized from hot ethanol in large (2−3 mm), soft crystals. One of these was cut to create a suitable specimen. Compound **4** crystallized from hot *p*-xylene in comparatively hard and brittle needlelike crystals. A crystal of **1** was mounted on a Bruker-AXS SMART APEX CCD-equipped diffractometer, while those of **2**, **3**, and **4** were measured on an Enraf-Nonius Mach3 serial diffractometer. Molecular structures and atomic numbering for these compounds can be found in Figures 1 and 2; hydrogen atoms are given the same number as the carbon atom they are substituted on. Data reduction was done with SAINT+[10] for **1** and XCAD4[11] for **2**−**4**. The structures were solved and refined with SHELX97.[12] Details of the data collection and structure refinement can be found in Table 1. For the four compounds, the initial hydrogen positions were calculated. All the atoms of compound **1**, including hydrogen, were allowed to refine freely. In compounds **2** and **3**, the terminal methyl groups were restrained with the SHELX AFIX 138 command, which allows methyl rotation and refinement of the bond length. For compound **3**, the hydrogens in the five methylene groups of the hexyl chain were also restrained with AFIX 24. For compound **4**, the hydrogens in the ethoxy fragment of the side chain were refined freely, but to retain a reasonable geometry, it was necessary to fix H14 and H15 in ring C (see Figure 2d) with HFIX 43. Additionally, the methyl groups were kept restrained with AFIX 138. The limits for observing short contacts were chosen at the van der Waals radii[13] of the participating atoms, unless indicated otherwise. The crystal structures have been deposited at the Cambridge Crystallographic Data Centre with reference numbers 221853 (**1**), 221854 (**2**), 221855 (**3**), and 221856 (**4**).

Theoretical calculations on compound **1** were performed using the Gaussian 98 suite of programs[14] at the DFT/B3LYP level of theory using the 6-31G* basis set, starting from AM1 optimized geometries. The basis set was used as it is implemented in the program. Geometries and energies were calculated for the three possible conformers of compound **1** given in Figure 7: both the [*sp*,*sp*] and the [*ap*,*ap*] conformers were calculated in C_2 symmetry and the [*sp*,*ap*] conformer was calculated in C_1 symmetry. Due to the size of the molecules, no frequency calculations were performed to verify that the two C_2 conformations are energy minima. Cartesian coordinates and energies of the calculated structures can be found in the Supporting Information.

3. Results and Discussion

3.1. Description of the Four Crystal Structures. For all of the structures described here, the asymmetric unit is half of a molecule. *E*,*E*-1,4-Bis[2-(2,4,6-trimethoxyphenyl)ethenyl]-2,5-dimethoxybenzene (**1**) crys-

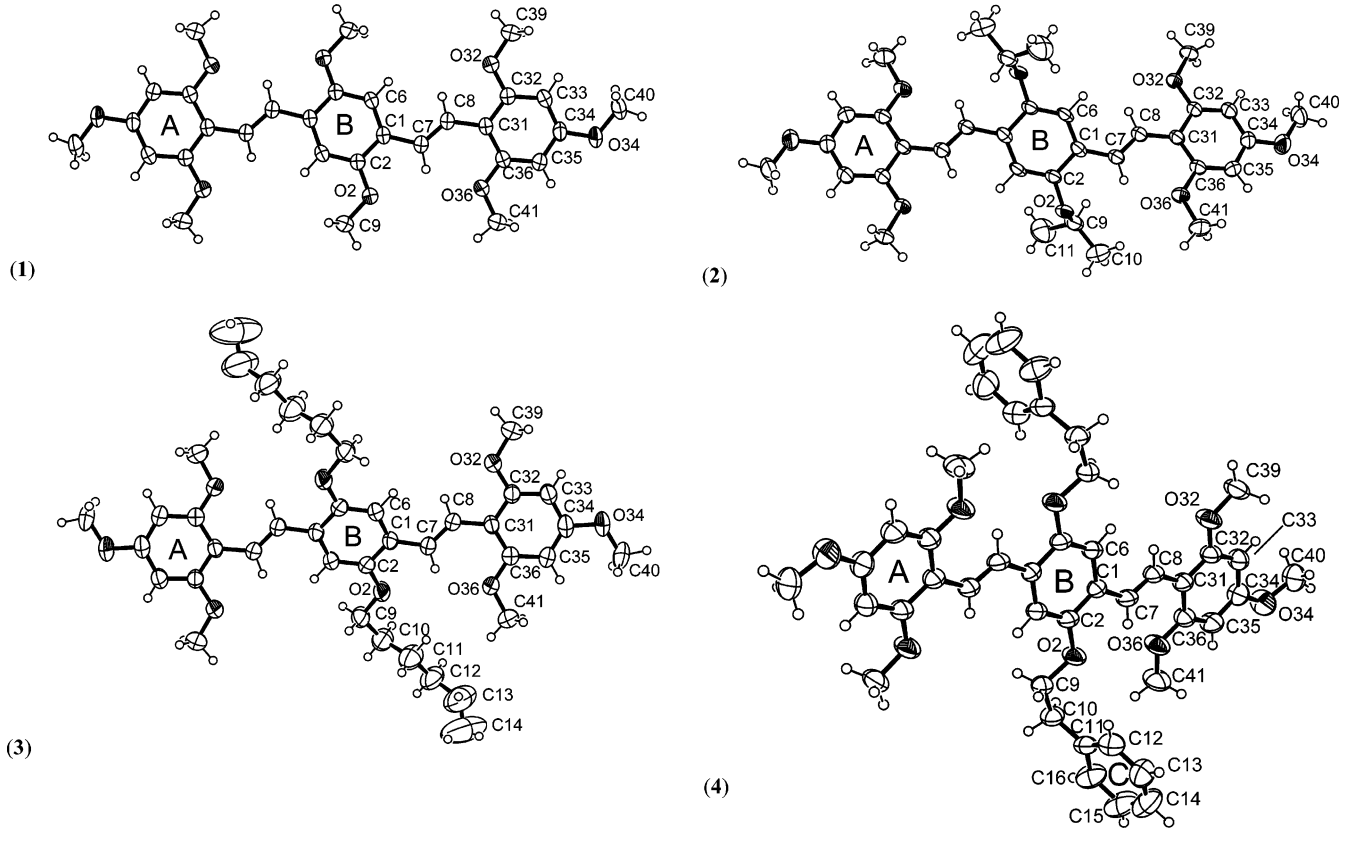

Figure 2. Molecular structure and atomic numbering of **1**, **2**, **3**, and **4**. Displacement ellipsoids are at the 50% probability level; hydrogens are represented by spheres of arbitrary radius.

Table 1. Details of Data Collection and Refinement for the Four Compounds

	1	**2**	**3**	**4**
		A. Crystal Data		
chemical formula	$C_{30}H_{34}O_8$	$C_{34}H_{42}O_8$	$C_{40}H_{54}O_8$	$C_{44}H_{46}O_8$
formula weight ($g \cdot mol^{-1}$)	522.57	578.68	662.83	702.81
cell setting	triclinic	triclinic	monoclinic	triclinic
space group	$P\bar{1}$	$P\bar{1}$	$P2_1/c$	$P\bar{1}$
radiation type	Mo Kα	Mo Kα	Mo Kα	Mo Kα
wavelength (Å)	0.710 73	0.710 73	0.710 73	0.710 73
monochromator	graphite	graphite	graphite	graphite
crystal form	block	needle	block	needle
crystal size (mm^3)	0.34 × 0.30 × 0.20	0.36 × 0.26 × 0.15	0.36 × 0.36 × 0.28	0.35 × 0.30 × 0.10
crystal color	orange	orange	yellow	yellow
no. of reflns for cell param	2995	25	25	25
θ range (deg)	2.634−28.082	5.69−17.99	3.97−18.57	6.36−20.34
$F(000)$	278	310	716	374
T (K)	293	293	293	293
a (Å)	8.0838(9)	7.572(5)	8.174(2)	6.897(2)
b (Å)	8.9765(10)	9.033(5)	15.302(4)	9.628(2)
c (Å)	9.9412(11)	11.729(5)	16.320(4)	14.066(2)
V ($Å^3$)	676.82(13)	776.8(7)	1835.6(8)	918.6(4)
Z	1	1	2	1
D_x ($mg \cdot m^{-3}$)	1.282	1.237	1.199	1.270
μ (mm^{-1})	0.093	0.087	0.082	0.087
		B. Data Collection		
diffractometer	Bruker AXS SMART APEX CCD	Enraf-Nonius Mach3	Enraf-Nonius Mach3	Enraf-Nonius Mach3
data collection method	ω scans	$\omega/2\theta$ scans	$\omega/2\theta$ scans	$\omega/2\theta$ scans
no. of measured reflns	5693	3609	4243	4332
no. of independent reflns	2995	3352	3961	3989
no. of obsd reflns	2301	1689	1560	1553
criterion for obsd reflns	$I > 2\sigma(I)$	$I > 2\sigma(I)$	$I > 2\sigma(I)$	$I > 2\sigma(I)$
θ_{max} (deg)	28.25	26.98	26.98	26.96
range of h	$-10 \le h \le 10$	$0 \le h \le 9$	$0 \le h \le 10$	$0 \le h \le 8$
range of k	$-11 \le k \le 11$	$-11 \le k \le 11$	$-18 \le k \le 18$	$-12 \le k \le 12$
range of l	$-13 \le l \le 13$	$-14 \le l \le 14$	$0 \le l \le 19$	$-17 \le l \le 17$
no. of standard reflns		3	3	3
frequency of standard reflns (h)		1	1	1
intensity decay (%)	0	11	4	3
		C. Refinement		
refinement on	F^2	F^2	F^2	F^2
GOF	1.040	1.039	0.994	0.969
R_w	0.142	0.182	0.206	0.266
R_u	0.054	0.061	0.059	0.082
R_{all}	0.069	0.173	0.227	0.232
no. of reflns used in refinement	2995	3352	3961	3989
no. of params used	240	218	245	277
weighting scheme		$w = 1/[\sigma^2(F_o^2) + (AP)^2 + BP]$, where $P = (F_o^2 + 2F_c^2)/3$		
A	0.08	0.10	0.10	0.10
B	0.07	0.00	0.00	0.00
$(\Delta/\sigma)_{max}$	0.01	0.00	0.00	0.00
$\Delta\rho_{max}$	0.20	0.24	0.36	0.22
$\Delta\rho_{min}$	−0.26	−0.34	−0.34	−0.26

Table 2. Experimental (XRD) and Calculated (DFT) Values of the Torsion Angles τ (deg) between the Least-Square Planes through the Inner (B) and Outer Rings (A) and the Double Bond (DB)

method	compd	τ(A−DB)	τ(DB−B)	τ(A−B)
XRD	**1**	1.45(19)	8.2(2)	6.8(2)
	2	2.72(13)	24.7(4)	25.3(2)
	3	11.58(17)	14.1(3)	25.5(2)
	4	8.3(8)	3(1)	6.4(2)
DFT	**1**	5.41	12.97	18.28

tallizes in the space group $P\bar{1}$. It can be seen from the torsion angles between the different fragments of the molecule, which are given in Table 2, that the individual molecules are nearly planar with the olefinic links lying in the plane of the outer rings (A). A graphical representation of the structure is given in Figure 3, which indicates that the molecules stack in layers. The figure contains a section of the unit cell and shows that in every layer one of the two *ortho*-methoxy groups of the outer ring (A) lies above the centroid of the central ring (B) of the previous layer, and the methoxy groups of the central ring (B) are positioned above the centroids of the outer rings (A) of the molecules in the next and previous layers. We will call this arrangement "separate stacks" (see Figure 3). These interactions are given by H41b···Cg(B), symm code $1 - X, -Y, 1 - Z$, 2.686(18) Å, 153.6(14)° and H9b···Cg(A), symm code $X, 1 + Y, Z$, 2.79(3) Å, 147.8(18)°. The lowercase letter "b" indicates the second of the three hydrogen atoms on C9 of the

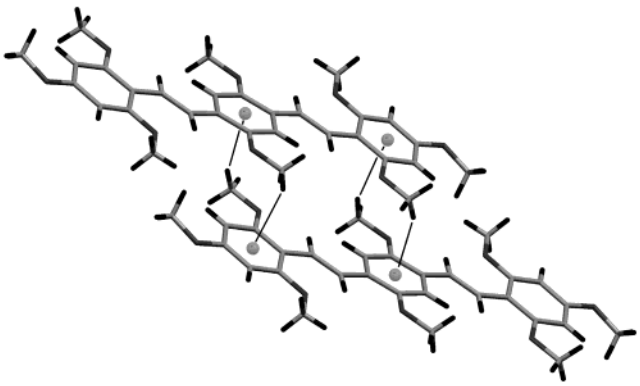

Figure 3. Graphical representation of the packing and $-OCH_3-\pi$ interactions in **1**.

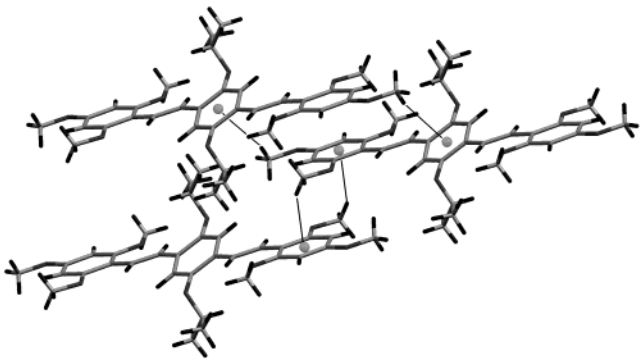

Figure 4. Graphical representation of the packing and the $-OCH_3-\pi$ network in **2**.

methyl group, while Cg(B) indicates the centroid of ring B. In the generic form of the expression "H···B, symm code, distance, angle", "angle" is defined as the angle C−H···B. These interactions have been indicated by the thin full lines in Figure 3. There also is a short contact between the same *ortho*-methoxy group of the outer ring (A) and C1 of the central ring (B) (not shown in Figure 3) given by H41b···C1, symm code $1 - X, -Y, 1 - Z$, 2.836(17) Å, 124.1(13)°. The stacks are side-to-side with the methoxy groups of adjacent stacks intercalated. There is a short contact between the hydrogen atoms of the methoxy groups on the central rings (B) of adjacent stacks (not shown in Figure 3) given by H9a···H9a, symm code $1 - X, 1 - Y, -Z$, 2.26(3) Å, 128.9(18)°. The noninteracting *ortho*- and *para*-methoxy groups of the outer rings (A) are grouped together between the stacks.

The unit cell of *E*,*E*-1,4-bis[2-(2,4,6-trimethoxyphenyl)ethenyl]-2,5-diisopropoxybenzene (**2**) is somewhat larger than the cell of **1** and differently proportioned, even though the space group is still $P\bar{1}$. The interactions governing the packing here have changed to accommodate the larger isopropoxy groups. Here, only $-OCH_3-\pi$ interactions seem to be available to determine the overall packing, and now they involve the *ortho*- and *para*-methoxy groups in the outer rings (A) only: the *para*-methoxy groups interact with ring B of the next layer in the same stack, and one of the *ortho*-methoxy groups with ring A of the next layer in the adjacent stack. We will call this arrangement "interconnected stacks" (see Figure 4). The interactions are given by H39c···Cg(A), symm code $-X, 1 - Y, 1 - Z$, 2.761(15) Å, 150.3(10)° and H40c···Cg(B), symm code $X, Y, 1 + Z$ and $1 - X, 1 - Y, 1 - Z$, 2.884(16) Å, 146.9(13)°. They have been represented by the thin full lines in Figure 4. The result of the simultaneous presence of these two interactions is not only that the framework has become three-dimensional, but also that it is more spread out. The central rings are tilted out of their original planes by the isopropoxy substituents. These groups are, together with the noninteracting *ortho*-methoxy groups of the peripheral rings (A), still positioned between the layers, analogous to the packing of **1**. Equally, as Table 3 shows, the tilting of the central ring out of the plane has lengthened the interactions between the hydrogen atoms on the olefinic link, H7 and H8, and the oxygen atoms on the methoxy groups, O2, O32, and O36, which are designated CH−*n*(O).[15] Furthermore, three short interactions (not shown in Figure 4) with distances shorter than the sum of the van der Waals radii of the participating atoms, now exist between one 2-methoxy group on the peripheral ring (A) and a carbon atom from the same ring in the next layer of the next stack (not shown in Figure 4) given by H39c···C34, symm code $-X, 1 - Y, 1 - Z$, 2.880(15) Å, 122.6(9)° between C7 of the olefinic link and H11b of the molecule two layers away in the next stack given by H11b···C7, symm code $1 + X, Y, Z$, 2.883(17) Å, 132(2)° and between H39b and H35 of the molecule two stacks away given by H39b···H35, symm code $X, 1 + Y, Z$, 2.33(3) Å, 168(2)°.

Table 3. Experimental (XRD) and Calculated (DFT) CH−*n*(O) Distances, *r* (Å), between the Hydrogen Atoms on the Olefinic Link and the Oxygen Atoms of the Methoxy Groups and Angles, α (deg), between the Olefinic CH Bond and the Oxygen Atom of the Nearest Methoxy Group[a]

		H7···O2 five-membered		H8···O32 five-membered		H7···O36 six-membered	
method	compd	*r*	α	*r*	α	*r*	α
XRD	**1**	2.34(2)	101.16	2.16(1)	107.86	2.18(1)	117.17
	2	2.52(3)	95.70	2.25(2)	101.03	2.15(3)	118.31
	3	2.33(3)	99.57	2.23(3)	103.23	2.19(3)	115.49
	4	2.26(4)	101.13	2.21(4)	105.23	2.05(5)	123.00
DFT	**1**	2.33	100.5	2.21	105.3	2.18	117.2

[a] Original values of *r* and α were corrected by a normalization of the CH bond lengths to 1.083 Å.

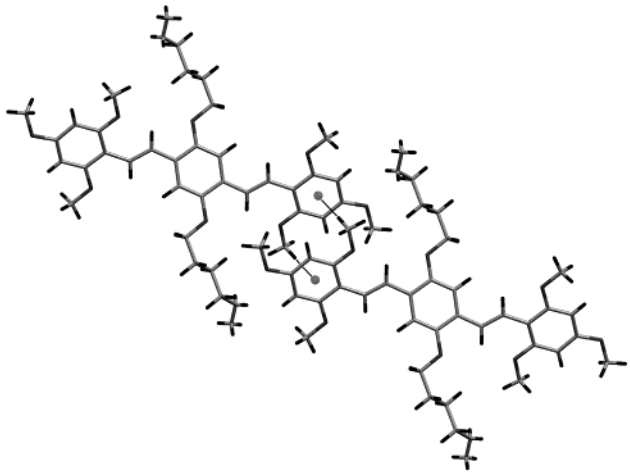

Figure 5. Graphical representation of the packing and $-OCH_3-\pi$ interactions in **3**.

E,*E*-1,4-Bis[2-(2,4,6-trimethoxyphenyl)ethenyl]-2,5-dihexoxybenzene (**3**) crystallizes in the monoclinic space group $P2_1/c$, and it displays a very different kind of packing. The arrangements that were observed for compounds **1** [separate stacks with the alkoxy chains placed between] and **2** [interconnected stacks] are no longer present here. Hexoxy chains are now completely surrounding the central rings and the olefinic links of the oligomers. The only methoxy−Cg interactions still present are contacts between one *ortho*-methoxy group of the peripheral rings (A) and a peripheral ring (A) in the next layer, as can be seen in Figure 5. These interactions link the molecules into "strings" that have only little interaction with the others around them. A further expression of this formation of strings can be found in the close contacts between the two adjacent peripheral rings (A) of two molecules within the string (not shown in Figure 5) given by Cg(A)···Cg(A), symm code $1 - X, -Y, 1 - Z$, 4.883(2) Å, 3.687 Å perp. The

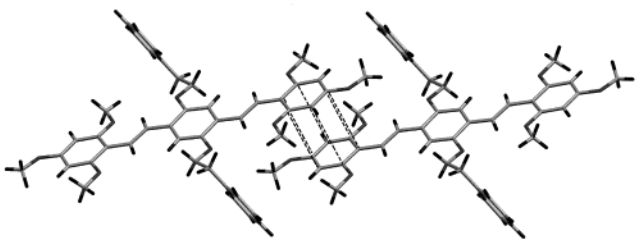

Figure 6. Graphical representation of the packing and $-OCH_3-\pi$ interactions in **4**.

distance designated by "perp" is the perpendicular distance from the centroid of one ring to the plane of the other.

There are no other intermolecular contacts with surrounding molecules that are shorter than the sum of the van der Waals radii of the atoms concerned. Equally, the $-OCH_3-\pi$ contacts have grown much weaker here. Those that are still present are 0.3−0.5 Å longer than those in the two structures presented above, possibly due to the steric requirements of the side chains. The shortest one is a methoxy contact between one 2-methoxy group of a peripheral ring (A) and a peripheral ring (A) in a next layer given by H41a···Cg(A), symm code $1 - X, -Y, 1 - Z$, 3.16(3) Å, 153.0(18)°, that is, within one "string". This interaction has been represented by the thin full lines in Figure 5. The other contacts can be found between hexoxy chains and aromatic rings in different "strings" (not shown in Figure 5), which are given by H11a···Cg(A), symm code $^3/_2 - X, {}^1/_2 - Y, -{}^1/_2 + Z$, 3.28(2) Å, 166.9(12)° and H14c···Cg(B), symm code $-{}^1/_2 + X, -{}^1/_2 + Y, {}^1/_2 - Z$, 3.32(9) Å, 167(11)°. It can be clearly seen in Figure 2c that the outer two carbons of the hexyl chain (C13 and C14) have very large displacement ellipsoids; the corresponding C−C distance is therefore not realistic [1.232(7) Å]. This can be due either to static or dynamic disorder of this part of the structure, but this was not further investigated. No restraints or constraints were imposed on these atoms to not divert attention from the problem. Due to this issue, the "close contact" of H14c to Cg(B) has to be approached with utmost care. The surprising lack of close contacts in the crystal structure of this oligomer, combined with its very easy crystallization, indicates that the molecular volume conforms so well to the requirements of neighboring molecules in exactly filling the available space and avoiding "stress areas" that additional stabilization by $-OCH_3-\pi$ interactions is unnecessary and indeed outweighed by these sterical considerations. This is also reflected in the slight decrease in density for **3**.

For *E*,*E*-1,4-bis[2-(2,4,6-trimethoxyphenyl)ethenyl]-2,5-bis(2-phenylethoxy)benzene (**4**), the crystal structure reverts to the space group $P\bar{1}$. There is no additional tilting of the middle ring with respect to **1**, but here the olefinic links are in the plane of the central ring (B) rather than in that of the outer ring (A), as can be seen from Table 2. The structure, given in Figure 6, shows stacking of the outer rings (A) of the oligomer; this interaction is represented by the dotted lines in Figure 6 and is given by Cg(A)···Cg(A), symm code $1 - X, 2 - Y, 1 - Z$, 3.840(3) Å, 3.606 Å perp. The phenyl rings in the side chains show a similar interaction (not shown in Figure 6) given by Cg(C)···Cg(C), symm code $1 - X, 1 - Y, -Z$, 4.983(4) Å, 3.688 Å perp. In this case, there are no methoxy groups positioned between the two rings, and thus the latter display a pure $\pi-\pi$ interaction, in contrast to structure **3** for which the formation of the "strings" is based on $-OCH_3-\pi$ contacts. In the case of **4**, additional stabilization is provided by a whole set of hydrogen$-\pi$ contacts, not unlike those reported in the precursor molecule 1,4-bis(2-phenylethoxy)-benzene.[16] The following hydrogen$-\pi$ interactions between the ethoxy fragment of the side chain and both the central rings (B) of the oligomer backbone and the rings (C) of the side chains could be distinguished: H9a···Cg(C), symm code $1 - X, 1 - Y, -Z$, 2.77(5) Å, 135(3)°; H10a···Cg(B), symm codes $-1 + X, Y, Z$ and $1 - X, 2 - Y, -Z$, 3.36(5) Å, 97(3)°; H10b···Cg(B), symm codes $-1 + X, Y, Z$ and $1 - X, 2 - Y, -Z$, 2.75(5) Å, 141(3)°. Finally, there exists a herringbone-type interaction between one of the side chain ring (C) protons and the peripheral ring (A) of the conjugated backbone given by H14···Cg(A), symm code $X, -1 + Y, Z$, 3.05(7) Å; 146(6)°.

Table 4. Components of the Libration (deg²) Obtained in the TLS Analysis of 1 and 2 and Angles β (deg) between the Three Libration Axes and the Long Axis of the Molecule

	L_1	L_2	L_3
1	12(3)	2.0(15)	1.3(11)
β	21.07	110.24	84.39
2	17(4)	4(2)	1.5(1)
β	12.49	99.91	97.31

3.2. General Description of the Packing of 1,4-Bis(α-styryl)benzene Derivatives. A number of features are common to the four structures, regardless of the space group they crystallize in. The bond lengths and angles contain no surprises. All four structures very clearly show the CH$-n$(O) interactions between the olefinic protons and the free electron pairs of the oxygen atoms of the methoxy groups in their vicinity, as can be seen in Table 3. For compounds **1** and **2**, the data and refinement allowed a Translation-Libration-Screw (TLS) analysis,[17,18] the results of which are shown in Table 4. This shows that the main rotational component lies along the long axis of the molecule, as expected, and is in both cases 1 order of magnitude larger than the other librations. The translations are close to isotropic.

On the other hand, several features are remarkably different for the four compounds. This is the case for the torsion angles between the rings and the double bonds (see Table 2). These are of particular interest when trying to assess the contributions of the different forces that try to keep the molecule planar (conjugation) and those that cause deformations from planarity (lattice effects due to the bulkiness of the side chains). An additional factor has been identified as the formally nonbonding CH$-n$(O); in principle, these interactions can either be attractive and work together to keep the molecule planar or become repulsive and generate enough steric hindrance between the methoxy groups on the rings and the olefinic hydrogen atoms that they force the molecular framework away from planarity.

The theoretical calculations performed on compound **1** provide an objective basis from which one can try to elucidate the precise effect of the CH$-n$(O) interactions on the overall geometry and their importance in comparison with the other forces. These calculations show

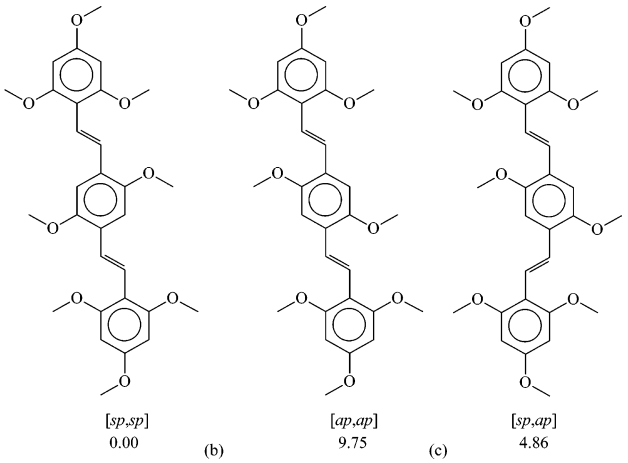

Figure 7. Calculated conformers of **1**. IUPAC names and relative energies (kJ·mol^{-1}) are given. See text for the nomenclature of the conformers.

that the most stable conformer of **1** is the one in which the double bonds are positioned anti with respect to one another and the methoxy groups of the central ring are directed toward both H7 atoms on the double bonds. Figure 7 shows the three possible conformers for **1**, their IUPAC names, and their relative energies. This most stable conformer, designated [*sp*,*sp*] in Figure 7a, displays six CH−*n*(O) interactions in four five-membered and two six-membered ring configurations. Comparison with the conformer with the double bonds syn, designated [*sp*,*ap*] in Figure 7c, which displays three five-membered and three six-membered ring interactions, and the second anti conformer with the central ring twisted over 180°, designated [*ap*,*ap*] in Figure 7b, which displays two five-membered and four six-membered ring interactions, reveals that the replacement of a five-membered by a six-membered ring interaction raises the energy of the molecule by 4.86 kJ·mol^{-1}. The most stable anti conformer, [*sp*,*sp*] (Figure 7a), is the one found in the crystal for all compounds discussed here. Even though these data suggest that the five-membered CH−*n*(O) interactions have a stabilizing effect, it is difficult to separate this from the effects of the six-membered ring interactions or steric effects. We refer to results from one of our earlier publications on the crystal structure of *E*,*E*-1,4-bis[2-(2,4-dimethoxyphenyl)ethenyl]-2,5-dimethoxybenzene, to quantify the effects of torsion on the CH−*n*(O) interactions.[19] The work we presented there clearly indicates that the torsion potential well of the central ring of an oligomer flanked by two five-membered ring CH−*n*(O) interactions is steeper than that of the same ring with only one such interaction. This points to an attractive interaction. We do, however, note that the potential well is relatively flat, and up to a torsion angle of 20° away from the minimum energy conformation, the energy difference remains small. This corroborates the observation that the rings can be twisted out of the plane of the double bond as far as they do for compounds **1**−**4** to accommodate the larger side chains without having a negative impact on the overall stabilization of the molecule.

The determining factor in the packing of the four 1,4-bis[2-(2,4,6-trimethoxyphenyl)ethenyl]benzenes under investigation appears to be the −OCH$_3$−π contacts, a wide choice of which can exist due to the large number of methoxy groups and aromatic rings in different parts of the molecule. These weak interactions will become important when no other stronger stabilization for the structure is available. Furthermore, the systems presented here are ideally suited for displaying CH−π interactions since they feature both relatively acidic hydrogen atoms in the methoxy groups and electron-rich π-systems (substituted with electron-donating substituents) and lack other obvious lattice-determining interactions. A listing of all the −OCH$_3$−π contacts in structures **1**−**3**, together with their distances and angles, can be found in Table 5: distances *d*, between the hydrogen atom of the methoxy group and the centroid (Cg) of the appropriate benzene ring, and *D*, between the carbon atom of the methoxy group and the centroid (Cg) of the appropriate benzene ring, as well as the angle θ, between the CH bond vector and the line connecting the hydrogen atom of the methoxy group and the centroid (Cg) of the appropriate benzene ring, are presented. For compounds **1** and **2**, there are two different kinds of −OCH$_3$−π contacts: those to the central benzene ring (B) substituted with two methoxy and two ethenyl groups and those to the peripheral benzene ring (A) substituted with one ethenyl and three methoxy groups. The latter ring is more electron-rich, supposedly leading to a stronger interaction with the −OCH$_3$ group.[20] Indeed, when comparing the relevant distances and angles for compounds **1** and **2** in Table 5, the increase in both *d* and *D* can be clearly seen. Thus, the relatively weak −OCH$_3$−π interactions do appear to play an important role, which allows us to tentatively conclude that for compounds **1** and **2** they must also be the interactions that determine the lattice. The data in Table 5 also indicate that this is apparently not the case for compound **3**, where a −OCH$_3$−π interaction can be found that falls just outside the van der Waals cutoff criterion of 3.0 Å. The stacking of compound **3** is adversely affected by other factors, as will be discussed below.

Table 5. Relevant Data for the −OCH$_3$−π Interactions in Structures 1−3[a]

compd	interaction	total[b]	*d* [H−Cg(π)]	*D* [C−Cg(π)]	θ [CH···Cg(π)]
1	C41−H41b···Cg(B)	4	2.58	3.58	152
	C9−H9b···Cg(A)	4	2.74	3.70	147
2	C39−H39c···Cg(A)	4	2.70	3.67	150
	C40−H40c···Cg(B)	4	2.78	3.73	146
3	C41−H41a···Cg(A)	4	3.05	4.04	152

[a] The positions of the hydrogens were normalized at 1.083 Å. Distances *d* and *D* are given in Å and angles θ in deg. See text for details. [b] Total number of interactions per molecule (as donor or acceptor).

We find nearly all the possible combinations of interactions upon lengthening the side chain and thus increasing the volume of the structure. In **1**, *ortho*-methoxy groups on the peripheral ring (A) interact with the central rings (B), and the methoxy groups on the central rings (B) interact with the peripheral rings (A). In **2**, similar interactions exist between the *para*-methoxy groups of the peripheral rings (A) and the central rings (B) and *ortho*-methoxy groups on the peripheral ring (A) and the peripheral rings (A). In **3**, we only observe interactions between the *ortho*-methoxy groups of the peripheral rings (A) and the peripheral

rings (A). Increasing the length of the side chain pushes molecules apart along their main axes, so the "overlap" between the backbones (expressed in the number and the positions of the interactions) is reduced; the resulting gaps in the lattice are filled by the side chains. As these become more and more prominent in the packing, as is seen for compound **3**, the fraction of the molecular surface available for standard van der Waals stabilization increases, which can then result in the reduction of the influence of the $-OCH_3-\pi$ interactions and in the remaining ones being weakened because the interacting fragments are pushed apart because of steric hindrance.

It is likely that the three different central ring side chains discussed here (methoxy, isopropoxy, and hexoxy) are of optimal length and bulkiness for the three kinds of observed $-OCH_3-\pi$ networks to be formed and that side chains of a different length and size introduce too much strain on the resulting structure to be stable and generate long-range order. This is most likely the explanation why several of the other 2,5-dialkoxy-substituted 1,4-bis[2-(2,4,6-trimethoxyphenyl)ethenyl]-benzenes that we synthesized did not crystallize under the conditions and from the solvents used. This was the case for derivatives with ethoxy, propoxy, butoxy, pentoxy, isopentoxy, heptoxy, octoxy, and 2-cyclohexyl-ethoxy side chains on the central ring.[9] For compound **4**, there are no $-OCH_3-\pi$ contacts left: they have been replaced by a network of interactions of a different nature ($\pi-\pi$, herringbone, and ethoxy$-\pi$ interactions). In effect, the presence of the extra benzene rings in the side chains dramatically alters the packing strategy. These observations suggest that choosing the side chain carefully, in a way that an $-OCH_3-\pi$ network cannot be formed, and at the same time avoiding groups that encourage other interactions [such as the 2-phenylethoxy group in **4**] should significantly reduce crystallization phenomena in a thin polymer blended film, as is used in devices such as OLEDs.

The values of the melting points of compounds **1**−**4**[9] agree well with the ideas on the interactions in the respective crystal structures presented above. Compounds **1**−**3** form a series with progressively lower melting points: compound **1** has the highest melting point (207−209 °C), and this value differs from the one of compound **2** (195−198 °C) by only 11 °C. The latter is 26 °C larger than the value of the melting point of compound **3** (170−171 °C), which is more than twice the previous difference. This is in accordance with the interactions in the crystal: compounds **1** and **2** display interactions that are comparable in number and strength (see Table 5), while the interactions in the lattice of compound **3** are fewer and weaker. Compound **4** (188−191 °C) does not fit in the series due to the different nature of its interactions, that is, $\pi-\pi$-stacking and herringbone interactions of the phenyl rings. The above also holds for the densities of compounds **1**−**3**: as the number of interactions decreases, so does the density (see Table 1).

As was mentioned in the Introduction, a review of several packing modes of a number of distyrylbenzenes, combined with new work in the field, has been published by Bartholomew and co-workers.[8] From the work presented here, it becomes equally clear that the distyryl-benzene moiety is extremely flexible. In the absence of good crystal synthons [which are absent in the structures **1**−**3**], the molecules have great difficulty forming larger crystals: the possible interactions leading to crystallization and aggregation, which include the $-OCH_3-\pi$ interactions, C═CH$-\pi$ interactions, PhH$-\pi$ herringbone, and $\pi-\pi$ interactions, are very weak and in fierce competition with each other. All of these are important contributors to the stability of these structures and lattices and are heavily influenced by the overall van der Waals contact stabilization and steric considerations. This means that small changes in the structure−such as an extra methyl group at the end of an alkoxy chain−can lead to very large differences in the packing, and if the free energy difference between different crystal morphologies is not large enough, this may lead to heavily disordered or even amorphous structures.

On one hand, this indicates that to use 1,4-bis(α-stryryl)benzenes as models for PPV type polymers, it is absolutely mandatory to identically copy the polymer substitution pattern in the model compound, and even then the validity of the obtained results will be doubtful at best. On the other hand, the extreme dependence of the crystal structure on the substitution of the molecule allows a substantial chance of finding compounds of this type that do not form large aggregates at all and would therefore be highly advantageous in terms of electronic devices based on amorphous layers. Unfortunately, until the advent of theoretical methods that can describe these weak interactions in sufficient detail for extended systems such as molecular crystals, it is difficult to predict *which* compounds to synthesize, and empirical observation remains our best tool.

4. Conclusions

The precise geometrical features of the separate molecules in the crystal phase of compounds **1**−**4**, such as the torsion angles between the central and peripheral rings and the olefinic link, are mainly determined by packing interactions in the crystal and not by intramolecular influences such as the CH$-n$(O) interaction. Three different $-OCH_3-\pi$ interaction patterns appear to determine the packing of 2,5-dialkoxy-substituted *E*,*E*-1,4-bis[2-(2,4,6-trimethoxyphenyl)ethenyl]benzenes, when other and more influential crystal structure synthons (such as the 2-phenylethoxy group) are absent. Steric considerations such as the length of the alkoxy side chains are extremely important and determine whether long-range crystallization occurs at all. This knowledge is invaluable when it comes to finding typically amorphous 1,4-bis(α-styryl)benzene derivatives for application in an electronic device, such as an OLED.

Acknowledgment. C.V.V. thanks the Fund for Scientific Research, FWO-Vlaanderen, for a grant as a research assistant. L.J.C. acknowledges support from FWO-Vlaanderen under Grant No. V4.039.01N. M.Z. was supported by NSF Grant 0111511, and the Bruker AXS Smart Apex diffractometer was funded by NSF Grant 0087210, by Ohio Board of Regents Grant CAP-491, and by YSU. F.B. acknowledges financing in the form of a research mandate from the Institute for the Promotion of Innovation through Science and Technology in Flanders (IWT-Vlaanderen).

Supporting Information Available: Crystallographic information in the form of CIF files, containing the atomic coordinates, the molecular geometry and ADPs for compounds **1**−**4** as well as additional information about the crystals and the experimental conditions, and Cartesian coordinates and energies of the calculated structures. This material is available free of charge via the Internet at http://pubs.acs.org.

References

(1) Tachelet, W.; Jacobs, S.; Ndayikengurukiye, H.; Geise, H. J.; Grüner, J. *Appl. Phys. Lett.* **1994**, *64*, 2364.
(2) Yang, J. P.; Heremans, P. L.; Hoefnagels, R.; Tachelet, W.; Dieltiens, P.; Blockhuys, F.; Geise, H. J.; Borghs, G. *Synth. Met.* **2000**, *108*, 95−100.
(3) Yang, J. P.; Jin, Y. D.; Heremans, P. L.; Hoefnagels, R.; Dieltiens, P.; Blockhuys, F.; Geise, H. J.; Van der Auweraer, M.; Borghs, G. *Chem. Phys. Lett.* **2000**, *325*, 251−256.
(4) Allen, F. H. *Acta Crystallogr.* **2002**, *B58*, 380−388.
(5) Bruno, I. J.; Cole, J. C.; Edgington, P. R.; Kessler, M.; Macrae, C. F.; McCabe, P.; Pearson, J.; Taylor, R. *Acta Crystallogr.* **2002**, *B58*, 389−397.
(6) Wallet, J.-C.; Molins, E.; Miravitlles, C. *Acta Crystallogr.* **2001**, *E57*, o1073−o1074.
(7) Wolska, I.; Poplawski, J.; Lozowicka, B. *Pol. J. Chem.* **1998**, *72*, 2331.
(8) Bartholomew, G. P.; Bazan, G. C.; Bu, X. H.; Lachicotte, R. J. *Chem. Mater.* **2000**, *12*, 1422−1430.
(9) Nowaczyk, J.; Chen, L.-J.; Baeke, J. K.; Moens, M.; Dieltiens, P.; Geise, H. J.; Van Alsenoy, C.; Blockhuys, F. *J. Electroanal. Chem.*, submitted for publication.
(10) Bruker, *SAINT+*, v6.02; Bruker AXS, Inc.: Madison, WI, 1997−1999.
(11) Harms, K. *XCAD4: Program for the Lp-correction of CAD4/Mach3 Diffractometer Data*; University of Marburg: Marburg, Germany, 1996.
(12) Sheldrick, G. M. *SHELX97 Programs for Crystal Structure Analysis*, release 97.2; University of Göttingen: Göttingen, Germany, 1997.
(13) Bondi, A. *J. Phys. Chem.* **1964**, *68*, 441.
(14) Frisch, M. J.; Trucks, G. W.; Schlegel, H. B.; Scuseria, G. E.; Robb, M. A.; Cheeseman, J. R.; Zakrzewski, V. G.; Montgomery, J. A., Jr.; Stratmann, R. E.; Burant, J. C.; Dapprich, S.; Millam, J. M.; Daniels, A. D.; Kudin, K. N.; Strain, M. C.; Farkas, O.; Tomasi, J.; Barone, V.; Cossi, M.; Cammi, R.; Mennucci, B.; Pomelli, C.; Adamo, C.; Clifford, S.; Ochterski, J.; Petersson, G. A.; Ayala, P. Y.; Cui, Q.; Morokuma, K.; Malick, D. K.; Rabuck, A. D.; Raghavachari, K.; Foresman, J. B.; Cioslowski, J.; Ortiz, J. V.; Stefanov, B. B.; Liu, G.; Liashenko, A.; Piskorz, P.; Komaromi, I.; Gomperts, R.; Martin, R. L.; Fox, D. J.; Keith, T.; Al-Laham, M. A.; Peng, C. Y.; Nanayakkara, A.; Gonzalez, C.; Challacombe, M.; Gill, P. M. W.; Johnson, B. G.; Chen, W.; Wong, M. W.; Andres, J. L.; Head-Gordon, M.; Replogle, E. S.; Pople, J. A. *Gaussian 98*, revision A.7; Gaussian, Inc.: Pittsburgh, PA, 1998.
(15) Blockhuys, F.; Hoefnagels, R.; Peten, C.; Van Alsenoy, C.; Geise, H. J. *J. Mol. Struct.* **1999**, *485*−*486*, 87−96.
(16) Vande Velde, C. M. L.; Baeke, J. K.; Geise, H. J.; Blockhuys, F. *Acta Crystallogr.* **2003**, *E59*, o828−o848.
(17) Shomaker, V.; Trueblood, K. N. *Acta Crystallogr.* **1968**, *B24*, 63.
(18) Spek, A. L. *PLATON: a multipurpose crystallographic tool*; Utrecht University: Utrecht, The Netherlands, 2003.
(19) Wu, G.; Jacobs, S.; Lenstra, A. T. H.; Van Alsenoy, C.; Geise, H. J. *J. Comput. Chem.* **1996**, *17*, 1820−1835.
(20) Nishio, M.; Minoru, H.; Yogi, U. In *The CH-π interaction*; Marchard, A. P., Ed.; Wiley VCH: New York, 1998; pp 62−63 and references therein.

CG0499764